Available online at www.sciencedirect.com
ScienceDirect
Mechanism and Machine Theory 42 (2007) 429–441
Mechanism and Machine Theory
www.elsevier.com/locate/mechmt

Experimental determination of instantaneous screw axis in human motions. Error analysis

Álvaro Page [a], Vicente Mata [b,*], Juan Víctor Hoyos [b], Rosa Porcar [a]

[a] *Instituto de Biomecánica de Valencia, Spain*
[b] *Departamento de Ingeniería Mecánica y de Materiales, Universidad Politécnica de Valencia, Camino de Vera s/n., 46022 Valencia, Spain*

Received 27 May 2005; received in revised form 23 March 2006; accepted 6 April 2006
Available online 8 June 2006

Abstract

The location of the instantaneous screw axis (ISA) is essential in order to obtain useful kinematic models of the human body for applications such as prosthesis and orthoses design or even to help in disease diagnosis techniques. In this paper, dual vectors will be used to represent and operate with kinematic screws with the purpose of locating the instantaneous screw axes which characterize this instantaneous motion. A photogrammetry system based on markers will be used to obtain the experimental data from which the kinematic magnitudes will be obtained. A comprehensive analysis of the errors in the measurement of kinematic parameters has been developed, obtaining explicit expressions for them based on the number of markers and their distribution. Finally, the developed methodology has been applied to the experimental determination of the *ISA* during an alternative motion of flexion and extension of the back.

Keywords: Instantaneous screw axis; Dual vectors; Biomechanics

1. Introduction

Most of the human body joints cannot be accurately modelled as lower kinematic joints. For this reason, the location of the instantaneous screw axis (*ISA*) is fundamental in order to generate a kinematic model of the human body which is able to reproduce its movement with the degree of accuracy needed in applications such as prostheses and orthoses design or in diagnosis techniques [5,7,8].

Experimental measurement of magnitudes such as the pose and velocity of mechanical systems implies a certain difficulty, which is greatly increased in the case of the human body, where there are some experimental limitations involved in measuring the 3D kinematics of the body segments without interferring with the spontaneous motion. Among the present techniques for experimental measurement of human movements, the

* Corresponding author. Tel.: +34 96 387 7621; fax: +34 96 387 7629.
E-mail address: vmata@mcm.upv.es (V. Mata).

0094-114X/$ - see front matter © 2006 Elsevier Ltd. All rights reserved.
doi:10.1016/j.mechmachtheory.2006.04.001

technique based on photogrammetry shows advantages for both the precision of the results and the non-interference with body motion.

The methods of human movement analysis based on photogrammetry usually describe the pose of a given body segment by means of a set of markers rigidly attached to it. The motion of the segment is determined by the changes in the markers coordinates between successive locations. There are some methods to analyze finite or infinitesimal displacements_from markers coordinates' changes. Most of them describe the motion from the translation of the centroid of the marker set, and its rotation, expressed by means of the corresponding rotation matrix [4,12].

At this point it is worth emphasizing that the representation of the motion of a rigid solid in space by means of screws has been applied for many years in an effective way to the mechanisms kinematic analysis [1–3]. Generally, two procedures have been used to represent screws: Plücker coordinates (Plücker Coordinates Representation) and dual vectors (Dual-vector Representation). Despite the wide use of the dual representation of screws in the field of Mechanisms and Machines Theory, and particularly in Robotics, it should be noted that the applications in the field of Biomechanics are limited and do not take full advantage of the possibilities that the concept of screw and its representation offer by means of dual vectors [6,10].

Independently of the procedure used to represent the movement of the corporal segments, the main problem that arises in the analysis of the human body motion corresponds to the error associated with the experimental measurement of the marker coordinates, and in the way that such error affects the determination of the linear and angular velocities and the location of the ISA. This problem has been dealt with, although in a more simplified way, in [11].

In this paper, a formulation for the kinematic analysis of human movements considering screws expressed in terms of dual vectors is presented. The proposed method determines the kinematic variables of the instantaneous movement (velocity, angular velocity and the position of the instantaneous axis of rotation) by using the markers coordinates in successive positions. This approach makes it possible to give a detailed analysis of the experimental errors associated with kinematic variables measurement, showing his skew-symmetric structure. Finally, the proposed method is validated by the experimental determination of the ISA in a given motion, and an application for the determination of the ISA corresponding to the movement of the back is shown.

2. Experimental determination of the kinematic screw by means of photogrammetry

2.1. Basic concepts and notation

Dual numbers are similar to the complex numbers with the complex unit i which has the property $\mathrm{i}^2 = -1$. But the dual unit ε is subjected to the rules:

$$\varepsilon \neq 0; \quad 0\varepsilon = \varepsilon 0 = 0; \quad 1\varepsilon = \varepsilon 1 = \varepsilon; \quad \varepsilon^2 = 0$$

The set of all dual numbers $\hat{a} = a_0 + \varepsilon a_1$, is a commutative ring having the numbers εa_1 as divisors of zero. Both a_0 and a_1 are real numbers; they are the so-called primal and dual part of the dual number $\hat{a}$, respectively [14].

A dual vector is quite similar to a three-dimensional vector, but replacing real components by dual numbers. This way, a dual vector $\hat{\mathbf{q}}$ can be expressed as

$$\hat{\mathbf{q}} = \begin{bmatrix} q_x + \varepsilon s_x \\ q_y + \varepsilon s_y \\ q_z + \varepsilon s_z \end{bmatrix} = \begin{bmatrix} q_x \\ q_y \\ q_z \end{bmatrix} + \varepsilon \begin{bmatrix} s_x \\ s_y \\ s_z \end{bmatrix} = \vec{\mathbf{q}} + \varepsilon \vec{\mathbf{s}}$$

Dual vectors are a useful mathematical tool to describe screws associated with the field of moments of a vector. Thus, given a vector $\vec{\mathbf{f}}$ located at the point A, its moment with respect to the origin of coordinates, O, can be calculated as $\vec{\mathbf{m}} = \vec{\mathbf{r}} \times \vec{\mathbf{f}}$, where $\vec{\mathbf{r}}$ is the position vector of A with respect to O. These two vectors can be combined into the dual vector: $\hat{\mathbf{f}} = \vec{\mathbf{f}} + \varepsilon \vec{\mathbf{m}}$. In this context, the dual unit ε has the dimension L^{-1}. In the same way, dual vectors can be used to represent lines, as an alternative to the Plücker coordinates. Thus, a straight line of unit vector **u** passing through point A may be represented as a dual vector $\hat{\mathbf{u}} = \vec{\mathbf{u}} + \varepsilon(\vec{\mathbf{r}} \times \vec{\mathbf{u}})$, being $\vec{\mathbf{r}}$ the position vector of A with respect to O.

The algebra of dual vectors is similar to that of three-dimensional usual vectors. The set of dual vectors is a module over the ring of dual numbers. A module is similar to a vector space with some differences, such as the torsion elements (vectors which are itself linearly dependent, for example a couple $\varepsilon\vec{\mathbf{m}}$). In [13] there is a good description of the algebraic structure of dual vectors applied to screws.

This approach is very useful to describe some mechanical magnitudes of a rigid body. This way, the instantaneous state of movement of a rigid body is specified by the angular velocity vector $\vec{\mathbf{w}}$ and the linear velocity of an arbitrary point A fixed in the body, $\vec{\mathbf{v}}_A$. These two vectors can be combined to make a dual vector called the dual velocity vector referring to point A, $\hat{\mathbf{w}} = \vec{\mathbf{w}} + \varepsilon\vec{\mathbf{v}}_A$ [13]. In the same way we can associate dual vectors to the linear momentum, $\vec{\mathbf{p}}$ and angular momentum with respect to a point A, $\vec{\mathbf{L}}_A$, by means of the dual momentum vector $\hat{\mathbf{p}} = \vec{\mathbf{p}} + \varepsilon\vec{\mathbf{L}}_A$. Finally, the dual force vector $\widehat{\mathbf{F}}$ includes the resultant external force, $\vec{\mathbf{F}}$ and the resultant external moment with respect to an arbitrary point A, $\vec{\mathbf{M}}_A$ acting in a rigid body, $\hat{\mathbf{F}} = \vec{\mathbf{F}} + \varepsilon\vec{\mathbf{M}}_A$ [15].

In this paper we will use the following notations:

$\hat{a}, \hat{v}, \hat{s}$: Italic character with circumflex represent dual numbers.
$\vec{\mathbf{v}}, \vec{\mathbf{w}}, \vec{\mathbf{F}}, \vec{\mathbf{r}}, \vec{\mathbf{R}}$: Bold character with arrow are three-dimensional vectors.
$\hat{\mathbf{r}}, \hat{\mathbf{w}}$: Bold character with circumflex, ^, are dual vector.
ε is the dual unit.
$\underline{\mathbf{A}}, \underline{\mathbf{M}}, \underline{\mathbf{J}}$: Underlined bold capital character are matrix.
$\widehat{\underline{\mathbf{A}}}, \widehat{\underline{\mathbf{M}}}, \widehat{\underline{\mathbf{J}}}$: Underlined bold capital character with circumflex, ^, are dual matrix.
A, P, G: Italic capital characters represent points. The letter G is reserved as the centroid of the marker set, in the sense of a mass centre.

2.2. Measurement of kinematic screw from markers coordinates

The systems of three-dimensional photogrammetry characterize the position and orientation of a rigid solid in space by using a set of three or more non-aligned markers associated to the solid. Although three points are enough to define the location of the solid, it is advisable to take more than three points for two reasons. In the first place to avoid indetermination in the position that would result if the solid hid one of the markers. The second problem is related to the experimental errors that can be committed, and that can be reduced by increasing the number of markers.

In Fig. 1, a rigid body and fixed reference system $\{O–XYZ\}$ are shown, the dual unit vectors associated to this reference system will be denoted as $\mathbf{B} = \{\hat{\mathbf{i}}, \hat{\mathbf{j}}, \hat{\mathbf{k}}\}$. On the rigid solid, N markers will have been considered P_i, $i = 1, 2, \ldots, N$. Let G be the centroid of the set of markers, whose position vector with respect to O is $\vec{\mathbf{r}}_G$. The dual unit vectors which define a reference system parallel $\{G–X'Y'Z'\}$ to the fixed one but having its their origin in the centroid of the distribution of markers associated to the body will be shown as $\mathbf{B}_G$. To each marker P_i a dual vector $\hat{\mathbf{r}}_i$, will be associated, corresponding to a screw whose central axis is the straight line GP_i and whose module is that of vector $\vec{\mathbf{r}}_i = \vec{\mathbf{r}}_{GP_i}$. Referred to $\mathbf{B}_G$ this dual vector has only a primal component, because all lines pass through G:

$$\hat{\mathbf{r}}_i = \vec{\mathbf{r}}_i + \varepsilon 0 \tag{1}$$

If the rigid body experiences a shift in the position at time dt, each one of the position screws $\hat{\mathbf{r}}_i$, will have been increased in d$\hat{\mathbf{r}}_i$.Considering the condition of rigid solid, d$\hat{\mathbf{r}}_i$ will be

$$\mathrm{d}\hat{\mathbf{r}}_i = \hat{\boldsymbol{\omega}} \times \hat{\mathbf{r}}_i \cdot \mathrm{d}t \tag{2}$$

because the module of $\hat{\mathbf{r}}_i$ is a constant [16]. The dual vector $\hat{\boldsymbol{\omega}}$ is the kinematic screw at time t. The cross-product which gives the expression (2) can be expressed by means of the corresponding skew-symmetric matrix $\widehat{\underline{\mathbf{A}}}_i$:

$$\hat{\boldsymbol{\omega}} \times \hat{\mathbf{r}}_i \,\mathrm{d}t = \widehat{\underline{\mathbf{A}}}_i \cdot \hat{\boldsymbol{\omega}}\,\mathrm{d}t \tag{3}$$

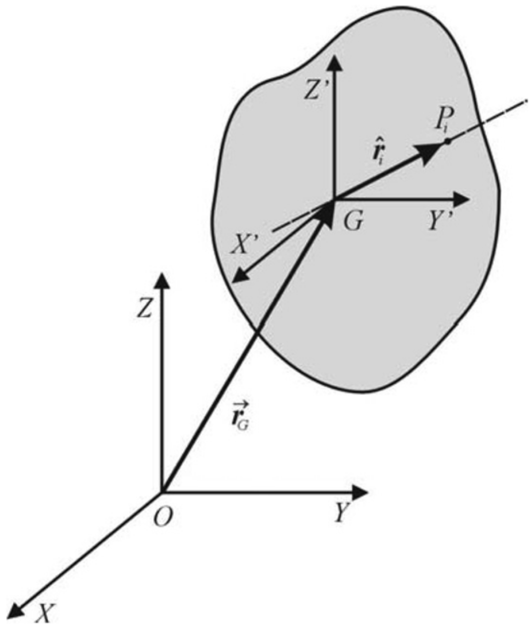

Fig. 1. Marker location representation with respect to the centroid of the set of the markers by means of dual vectors.

where

$$\underline{\widehat{\mathbf{A}}}_i = \begin{bmatrix} 0 & \hat{z}_i & -\hat{y}_i \\ -\hat{z}_i & 0 & \hat{x}_i \\ \hat{y}_i & -\hat{x}_i & 0 \end{bmatrix} \tag{4}$$

being $\hat{x}_i, \hat{y}_i, \hat{z}_i$ the components of $\hat{\mathbf{r}}_i$ in $\mathbf{B}_G$. Notice that the dual par of matrix $\underline{\widehat{\mathbf{A}}}_i$ is null, because we have chosen a reference system with centre in G. Extending the expression (2) to the N markers defined on the body and considering (3), it results in

$$\mathrm{d}\hat{\mathbf{r}} = \begin{bmatrix} \mathrm{d}\hat{\mathbf{r}}_1 \\ \mathrm{d}\hat{\mathbf{r}}_2 \\ \vdots \\ \mathrm{d}\hat{\mathbf{r}}_N \end{bmatrix} = \begin{bmatrix} \underline{\widehat{\mathbf{A}}}_1 \\ \underline{\widehat{\mathbf{A}}}_2 \\ \vdots \\ \underline{\widehat{\mathbf{A}}}_N \end{bmatrix} \hat{\boldsymbol{\omega}} \cdot \mathrm{d}t = \underline{\widehat{\mathbf{A}}} \cdot \hat{\boldsymbol{\omega}} \cdot \mathrm{d}t \tag{5}$$

By analysing the primal and dual part separately, Eq. (5) corresponds to a system of $6N$ equations (six components of $\mathrm{d}\hat{\mathbf{r}}_i$ for each marker) with six unknowns (the six elements of die kinematic screw). If there are three non-aligned markers, the system is compatible and determined, because both linear and angular velocity can be calculated from the velocities of three non-aligned points. With a higher number of markers, the measurement errors will invalidate the condition of rigid solid and the system will be incompatible, being able to be solved by means of the inverse generalized of matrix $\underline{\widehat{\mathbf{A}}}$:

$$\hat{\boldsymbol{\omega}} = (\underline{\widehat{\mathbf{A}}}^{\mathrm{T}} \cdot \underline{\widehat{\mathbf{A}}})^{-1} \underline{\widehat{\mathbf{A}}}^{\mathrm{T}} \cdot \frac{\mathrm{d}\hat{\mathbf{r}}}{\mathrm{d}t} \tag{6}$$

The solution obtained in (6) provides the value of $\hat{\boldsymbol{\omega}}$ which solves (5) in the sense of an adjustment by Least Squares method. Because Eq. (6) derives from (2), it imposes the rigid body constraint. In this way, those possible disturbances which might be derived from the experimental errors, Eq. (6) filters those that imply a modification in the distances between points and only allows the compatible solutions with rotations and the displacements of the corporal segment in block. In short, the permissible errors in the determination of the kinematic screw $\hat{\boldsymbol{\omega}}$ correspond to a skew-symmetrical field of displacements that verifies (2). That is to say, the only possible effect of the errors (due to the displacements of the skin or to errors in the coordinates of the markers) is equivalent to an additional kinematic screw (error screw), which is added to the screw of actual movement.

The expression (6) can be simplified if both sides are multiplied by $\underline{\widehat{\mathbf{A}}}^{\mathrm{T}} \cdot \underline{\widehat{\mathbf{A}}}$, with which will lead to

$$\underline{\widehat{\mathbf{A}}}^{\mathrm{T}} \cdot \underline{\widehat{\mathbf{A}}} \cdot \hat{\boldsymbol{\omega}} = \underline{\widehat{\mathbf{A}}}^{\mathrm{T}} \cdot \frac{\mathrm{d}\hat{\mathbf{r}}}{\mathrm{d}t} \tag{7}$$

On the other hand, bearing in mind that the dual part of $\underline{\widehat{\mathbf{A}}}$ is zero, it can be verified that

$$\underline{\hat{\mathbf{J}}} = \underline{\widehat{\mathbf{A}}}^{\mathrm{T}} \cdot \underline{\widehat{\mathbf{A}}} = \sum \underline{\mathbf{A}}_i^{\mathrm{T}} \underline{\mathbf{A}}_i = \underline{\mathbf{J}} = \begin{bmatrix} \sum(y_i^2 + z_i^2) & -\sum x_i \cdot y_i & -\sum x_i \cdot z_i \\ -\sum x_i \cdot y_i & \sum(x_i^2 + z_i^2) & -\sum y_i \cdot z_i \\ -\sum x_i \cdot z_i & -\sum y_i \cdot z_i & \sum(x_i^2 + y_i^2) \end{bmatrix} \tag{8}$$

$\underline{\mathbf{J}}$ can be interpreted as the tensor of inertia of the set of markers associated to the body as expressed in the reference system $\mathbf{B}_G$, considering a unitary mass in each one of the markers. Considering (8) and the meaning of matrix $\underline{\widehat{\mathbf{A}}}_i$ as a cross-product, Eq. (7) can be expressed as

$$\underline{\hat{\mathbf{J}}} \cdot \hat{\mathbf{w}} = \sum \hat{\mathbf{r}}_i \times \left(\frac{\mathrm{d}\hat{\mathbf{r}}_i}{\mathrm{d}t}\right) \tag{9}$$

The primal part of (9) is

$$\underline{\mathbf{J}} \cdot \vec{\mathbf{w}} = \sum \vec{\mathbf{r}}_i \times \left(\frac{\mathrm{d}\vec{\mathbf{r}}_i}{\mathrm{d}t}\right) \tag{10}$$

equation similar to that which relates the angular momentum of rigid body about its mass centre with the angular velocity, assuming that the markers have a unitary mass. Taking into account that the dual part of matrix $\underline{\hat{\mathbf{J}}}$ is null, it is evident that the dual part of Eq. (9) is

$$\mathrm{dual}\left(\sum \hat{\mathbf{r}}_i \times \left(\frac{\mathrm{d}\hat{\mathbf{r}}_i}{\mathrm{d}t}\right)\right) = \mathrm{dual}(\underline{\hat{\mathbf{J}}} \cdot \hat{\boldsymbol{\omega}}) = \underline{\mathbf{J}}.\vec{\mathbf{v}}_G \tag{11}$$

being $\vec{\mathbf{v}}_G$ the velocity of the centroid of the set of markers.

Definitively, the process used to calculate the kinematic screw is similar to the numerical calculation of kinetic screw, since the condition of rigid solid given by (2) implies the well-known relations between the kinetic screw and the kinematic screw. Actually, it is not necessary to obtain $\mathrm{d}\hat{\mathbf{r}}_i$, since Eq. (9) can also be written as

$$\hat{\mathbf{w}} = \vec{\mathbf{w}} + \varepsilon\vec{\mathbf{v}}_G = \underline{\hat{\mathbf{J}}}^{-1} \sum \hat{\mathbf{r}}_i \times \frac{\mathrm{d}\hat{\mathbf{r}}_i}{\mathrm{d}t} \tag{12}$$

expression that can be rewritten, based on the positions of the markers at time t, $\hat{\mathbf{r}}_i$, and $t + \mathrm{d}t$, $\hat{\mathbf{r}}_i' = \hat{\mathbf{r}}_i + \mathrm{d}\hat{\mathbf{r}}_i$, as follows:

$$\hat{\mathbf{w}}\,\mathrm{d}t = \underline{\hat{\mathbf{J}}}^{-1} \sum \hat{\mathbf{r}}_i \times (\hat{\mathbf{r}}_i' - \hat{\mathbf{r}}_i) \tag{13}$$

or

$$\hat{\mathbf{w}}\,\mathrm{d}t = \underline{\hat{\mathbf{J}}}^{-1} \sum \hat{\mathbf{r}}_i \times \hat{\mathbf{r}}_i' \tag{14}$$

explicit expression of the kinematic screw from two consecutive body positions. Once the screw is calculated, the determination of the orientation and location of the instantaneous screw axis is immediate.

3. Determination of experimental errors

The measurement of the markers displacement between two close locations is affected, fundamentally, by two sources of error: random experimental error associated to the accuracy of the measuring equipment and systematic error associated to the artifacts produced by skin displacements [17]. This paper deals with the random errors and their influence on the determination of the kinematic variables. Thus, the components of $\vec{\mathbf{r}}_i$ at a given time $(x_i y_i z_i)$ are assumed random variables with normal distributions of means $\bar{x}_i, \bar{y}_i, \bar{z}_i$ and standard deviations σ_x, σ_y, σ_z, respectively.

In order to analyze the propagation of experimental errors into $\hat{\mathbf{w}}$, we leave from Eq. (13). By differencing both sides of this equation we obtain:

$$\delta\hat{\mathbf{w}}\,\mathrm{d}t = \delta(\underline{\hat{\mathbf{J}}}^{-1})\sum\hat{\mathbf{r}}_i \times (\hat{\mathbf{r}}'_i - \hat{\mathbf{r}}_i) + \underline{\hat{\mathbf{J}}}^{-1}\sum\delta\hat{\mathbf{r}}_i \times (\hat{\mathbf{r}}'_i - \hat{\mathbf{r}}_i) + \underline{\hat{\mathbf{J}}}^{-1}\sum\hat{\mathbf{r}}_i \times (\delta\hat{\mathbf{r}}'_i - \delta\hat{\mathbf{r}}_i) \tag{15}$$

where $\delta\hat{\mathbf{w}}$ is the error in the measurement of $\hat{\mathbf{w}}$; $\delta\hat{\mathbf{r}}_i$ and $\delta\hat{\mathbf{r}}'_i$. represent the errors in the measurement of screws $\hat{\mathbf{r}}_i$ and $\hat{\mathbf{r}}'_i$, respectively. Eq. (15) can be simplified if we consider that we are analyzing infinitesimal displacements. Thus $\hat{\mathbf{r}}'_i - \hat{\mathbf{r}}_i$ is a first-order differential quantity and its product by another infinitesimal quantity is second-order differential. Therefore, the first and second terms of the right side of Eq. (15) are negligible with respect to the third one, and (15) can be rewritten as

$$\delta\hat{\mathbf{w}}\,\mathrm{d}t = \underline{\hat{\mathbf{J}}}^{-1}\sum\hat{\mathbf{r}}_i \times (\delta\hat{\mathbf{r}}'_i - \delta\hat{\mathbf{r}}_i) \tag{16}$$

or

$$\delta\hat{\mathbf{w}} = \left(\underline{\hat{\mathbf{J}}}^{-1}\sum\hat{\mathbf{r}}_i \times \frac{\delta\hat{\mathbf{r}}'_i}{\mathrm{d}t}\right) - \left(\underline{\hat{\mathbf{J}}}^{-1}\sum\hat{\mathbf{r}}_i \times \frac{\delta\hat{\mathbf{r}}_i}{\mathrm{d}t}\right) = \delta\hat{\mathbf{w}}_2 - \delta\hat{\mathbf{w}}_1 \tag{17}$$

The experimental error in the kinematic screw measurement has two components that correspond to the errors produced at initial position t, $\delta\hat{\mathbf{w}}_1$, and at the final position $t + \mathrm{d}t$, $\delta\hat{\mathbf{w}}_2$. These errors are screws that represent a fictitious motion between the actual and measured positions of the marker set. This movement is associated only to the part of the error in the markers positions that is compatible with the rigid body condition, since this verifies Eq. (12) and consequently (2). Thus it is that the measured motion between initial and final measured positions is equal to the resultant of the composition of three infinitesimal displacements (see Fig. 2). Firstly, at time t the body moves $-\delta\hat{\mathbf{w}}_1\,\mathrm{d}t$ from the measured position to the actual one. The second displacement is the motion $\hat{\mathbf{w}}\,\mathrm{d}t$ between actual positions at t and $t + \mathrm{d}t$. Finally, the effect of errors at final position is equivalent to a infinitesimal displacement $\delta\hat{\mathbf{w}}_2\,\mathrm{d}t$ between actual and measured positions at time $t + \mathrm{d}t$.

The components of $\delta\hat{\mathbf{w}}$ are random variables with null mean since they are a linear application of random variables with zero mean. In order to determine the standard deviation of its components, we analyze the component of the error screw $\delta\hat{\mathbf{w}}_1$, determined by means of the expression (17). The estimation of $\delta\hat{\mathbf{w}}_2$ can be made in the same way:

$$\delta\hat{\mathbf{w}}_1 = \underline{\hat{\mathbf{J}}}^{-1}\cdot\left(\sum\frac{\hat{\mathbf{r}}_i \times \delta\hat{\mathbf{r}}_i}{\mathrm{d}t}\right) \tag{18}$$

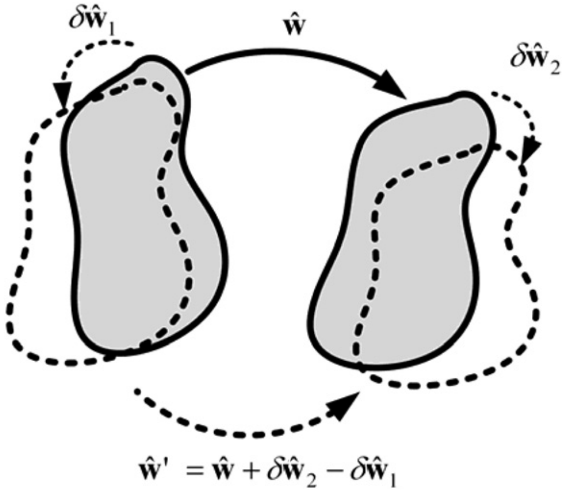

Fig. 2. Actual motion (solid lines) and observed motion as a consequence of error screws (dotted lines).

where $\hat{\underline{\mathbf{J}}}$ is the inertia tensor of the markers set with respect to a reference system with its origin in the centroid of the distribution of markers. If this reference system is chosen so that their axes are principal axes of inertia, it will lead to

$$\hat{\underline{\mathbf{J}}} = \begin{bmatrix} \lambda_1 & 0 & 0 \\ 0 & \lambda_2 & 0 \\ 0 & 0 & \lambda_3 \end{bmatrix} \quad \hat{\underline{\mathbf{J}}}^{-1} = \begin{bmatrix} \lambda_1^{-1} & 0 & 0 \\ 0 & \lambda_2^{-1} & 0 \\ 0 & 0 & \lambda_3^{-1} \end{bmatrix} \tag{19}$$

which greatly simplifies the calculation of $\delta\hat{\mathbf{w}}_1$. The primal part of (18) is

$$\delta\vec{\mathbf{w}}_1 = \hat{\underline{\mathbf{J}}}^{-1} \cdot \left(\sum \vec{\mathbf{r}}_i \times \frac{\delta\vec{\mathbf{r}}_i}{\mathrm{d}t} \right) \tag{20}$$

considering (20), it can be rewritten as

$$\begin{bmatrix} \delta w_{1x} \\ \delta w_{1y} \\ \delta w_{1z} \end{bmatrix} = \frac{1}{\mathrm{d}t} \begin{bmatrix} \frac{1}{\lambda_1} \sum(-z_i\,\delta y_i + y_i\,\delta z_i) \\ \frac{1}{\lambda_2} \sum(z_i\,\delta x_i - x_i\,\delta z_i) \\ \frac{1}{\lambda_3} \sum(-y_i\,\delta x_i + x_i\,\delta y_i) \end{bmatrix} \tag{21}$$

and supposing that the components of $\delta\vec{\mathbf{r}}_i$ are non-correlated normal distributions, with null mean and standard deviations a σ_x, σ_y, σ_z, the variances of the components of $\delta\vec{\mathbf{w}}_1$ will be

$$\begin{bmatrix} \sigma^2(w_{1x}) \\ \sigma^2(w_{1y}) \\ \sigma^2(w_{1z}) \end{bmatrix} = \frac{1}{\mathrm{d}t^2} \begin{bmatrix} \frac{1}{\lambda_1^2} \sum(z_i^2\sigma_y^2 + y_i^2\sigma_z^2) \\ \frac{1}{\lambda_2^2} \sum(z_i^2\sigma_x^2 + x_i^2\sigma_z^2) \\ \frac{1}{\lambda_3^2} \sum(y_i^2\sigma_x^2 + x_i^2\sigma_y^2) \end{bmatrix} \tag{22}$$

Finally, if the isotropy of the errors is admitted ($\sigma_x = \sigma_y = \sigma_z = \sigma$) the expression that provides the standard deviations of the components of the angular velocity, based on the errors in the position of the markers, is as follows:

$$\begin{bmatrix} \sigma(w_{1x}) \\ \sigma(w_{1y}) \\ \sigma(w_{1z}) \end{bmatrix} = \frac{1}{\mathrm{d}t} \begin{bmatrix} \frac{\sigma}{\sqrt{\lambda_1}} \\ \frac{\sigma}{\sqrt{\lambda_2}} \\ \frac{\sigma}{\sqrt{\lambda_3}} \end{bmatrix} \tag{23}$$

Expression (23) shows that the angular error in each principal direction is proportional to the standard deviation of the marker coordinates error. It depends on the inverse square root of the moment of inertia with respect to this principal axis. Therefore, the angular errors can be diminished by increasing the moment of inertia of the markers, which can be achieved either by increasing the number of markers or by separating its position so that it increases the turning radius with respect to the axis movement.

Considering now the dual part of (20), it is easy to see that

$$\delta\vec{\mathbf{v}}_G = \mathrm{dual}\left\{ \hat{\underline{\mathbf{J}}}^{-1} \cdot \left(\sum \frac{\hat{\mathbf{r}}_i \times \delta\hat{\mathbf{r}}_i}{\mathrm{d}t} \right) \right\} = \underline{\mathbf{J}}^{-1} \sum \frac{\vec{\mathbf{r}}_i \times \mathrm{dual}(\delta\hat{\mathbf{r}}_i)}{\mathrm{d}t} = \underline{\mathbf{J}}^{-1} \sum \frac{\vec{\mathbf{r}}_i \times (\delta\vec{\mathbf{r}}_G \times \vec{\mathbf{r}}_i)}{\mathrm{d}t} = \frac{\delta\vec{\mathbf{r}}_G}{\mathrm{d}t} \tag{24}$$

where $\delta\vec{\mathbf{r}}_G$ is the error on the measurement of the centroid of the marker set, G. The coordinates of G are calculated as a mean. Thus, according to the hypotheses proposed previously concerning the errors in marker coordinates, the standard deviations of the components of the error associated to the velocity of centroid G will be

$$\begin{bmatrix} \sigma(v_{Gx}) \\ \sigma(v_{Gy}) \\ \sigma(v_{Gz}) \end{bmatrix} = \frac{1}{\mathrm{d}t} \begin{bmatrix} \frac{\sigma}{\sqrt{N}} \\ \frac{\sigma}{\sqrt{N}} \\ \frac{\sigma}{\sqrt{N}} \end{bmatrix} \tag{25}$$

Expression that shows that the errors in the velocity of the centroid G depend both on the error of the markers coordinates and on the square root inverse of the number of markers. Therefore, the only way to diminish this error, for a given precision of the measurement system, is to increase the number of markers.

The expressions (23) and (25) provide the errors of the components of $\delta\hat{\mathbf{w}}_1$. Nevertheless, the error in the kinematic screw measurement, $\delta\hat{\mathbf{w}}$ depends both on $\delta\hat{\mathbf{w}}_1$ and $\delta\hat{\mathbf{w}}_2$ (see Eq. (17)). Therefore, supposing that the errors in the measurement of positions 1 and 2 are not correlated, the standard deviation of the error $\delta\hat{\mathbf{w}} = \delta\hat{\mathbf{w}}_2 - \delta\hat{\mathbf{w}}_1$, will be

$$\begin{bmatrix} \sigma(w_x) \\ \sigma(w_y) \\ \sigma(w_z) \end{bmatrix} = \frac{1}{\mathrm{d}t} \begin{bmatrix} \sigma\sqrt{\frac{2}{\lambda_1}} \\ \sigma\sqrt{\frac{2}{\lambda_2}} \\ \sigma\sqrt{\frac{2}{\lambda_3}} \end{bmatrix} \tag{26}$$

$$\begin{bmatrix} \sigma(v_x) \\ \sigma(v_y) \\ \sigma(v_z) \end{bmatrix} = \frac{1}{\mathrm{d}t} \begin{bmatrix} \sigma\sqrt{\frac{2}{N}} \\ \sigma\sqrt{\frac{2}{N}} \\ \sigma\sqrt{\frac{2}{N}} \end{bmatrix} \tag{27}$$

Once the error in the kinematic screw has been calculated, it is possible to determine its effect on the location of the instantaneous screw axis. In order to simplify the interpretation of the results, we have chosen the reference system shown in Fig. 3. Its Y-axis match the ISA, whereas the Z-axis should be perpendicular to the ISA and passing through the centroid of the markers bounded to the solid. In these conditions the measured kinematic screw $\hat{\mathbf{w}}'$ is the sum of the actual kinematic screw $\hat{\mathbf{w}}$, plus the error $\delta\hat{\mathbf{w}}$:

$$\hat{\mathbf{w}}' = \vec{\mathbf{w}}' + \varepsilon\vec{\mathbf{v}}'_O = \hat{\mathbf{w}} + \delta\hat{\mathbf{w}} = (\vec{\mathbf{w}} + \delta\vec{\mathbf{w}}) + \varepsilon(\vec{\mathbf{v}}_O + \delta\hat{\mathbf{v}}_G + \vec{\mathbf{r}}_{OG} \times \delta\hat{\mathbf{w}}) \tag{28}$$

The ISA will be the parallel straight line to $\vec{\mathbf{w}}'$ that goes through point H. If H is chosen so that OH is perpendicular to the ISA, then $\vec{\mathbf{r}}_{OH}$ can be calculated as

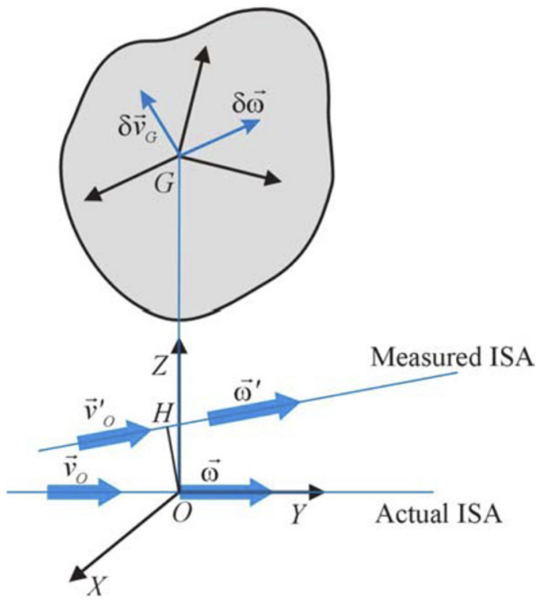

Fig. 3. Measured and actual ISA. The error in the kinematic screw propagates to the ISA direction (vector $\vec{\mathbf{w}}'$ instead of $\vec{\mathbf{w}}$) and location (point H).

$$\vec{\mathbf{r}}_{OH} = \frac{\vec{\mathbf{w}}' \times \vec{\mathbf{v}}'_O}{|\vec{\mathbf{w}}'|^2} \tag{29}$$

Bearing in mind (28), and neglecting second order differentials $\vec{\mathbf{r}}_{OH}$ becomes

$$\vec{\mathbf{r}}_{OH} \approx \frac{\vec{\mathbf{w}} \times \delta\vec{\mathbf{v}}_G}{w^2} + \frac{\delta\vec{\mathbf{w}} \times \vec{v}_G}{w^2} + \frac{\vec{\mathbf{w}}(\vec{\mathbf{r}}_{OG} \times \delta\vec{\mathbf{w}})}{w^2} \tag{30}$$

Eq. (30) demonstrates that $\vec{\mathbf{r}}_{OH}$ is made up of three terms:

- The first term is related to the error in the measurement of the velocity of the centroid G of the marker set:

$$(\vec{\mathbf{r}}_{OH})_1 = \frac{\vec{\mathbf{w}} \times \delta\vec{\mathbf{v}}_G}{w^2} = \frac{1}{\mathbf{w}}(\delta v_{Gz} \cdot \vec{\mathbf{i}} - \delta v_{Gx} \cdot \vec{\mathbf{k}}) \tag{31}$$

This error can be controlled by diminishing the components of $\delta\vec{\mathbf{v}}_G$ perpendicular to the ISA, which can be achieved by increasing either the number of markers or the accuracy of the measuring equipment.

- The second one is associated to the precision in the measurement of the angular velocity:

$$(\vec{\mathbf{r}}_{OH})_2 = \frac{\delta\vec{\mathbf{w}} \times \vec{\mathbf{v}}_O}{w^2} = \frac{v_O}{w^2}(-\delta w_z \cdot \vec{\mathbf{i}} + \delta w_x \cdot \vec{\mathbf{k}}) = p\left(\frac{-\delta w_z \cdot \vec{\mathbf{i}} + \delta w_x \cdot \vec{\mathbf{k}}}{w}\right) \tag{32}$$

As we can see, this term depends on the relation v_O/w, that is to say, on the pitch p of the kinematic screw. It is controlled by decreasing the error in the measurement of angular displacements, which can be achieved by increasing the inertia moment of the marker set or by improving the precision of measuring equipment. If movement is plane or spherical, then this term vanishes, because the pitch is null.

- Finally, the third one is

$$(\vec{\mathbf{r}}_{OH})_3 = \frac{\vec{\mathbf{w}} \times (\vec{\mathbf{r}}_{OG} \times \delta\vec{\mathbf{w}})}{w^2} = \left(\frac{\vec{\mathbf{w}} \cdot \delta\vec{\mathbf{w}}}{w^2}\right) \cdot \vec{\mathbf{r}}_{OG} = \frac{\delta w_y}{w} \cdot h \cdot \vec{\mathbf{k}} \tag{33}$$

This is a term of eccentricity that depends on the component of the angular error in the direction of the ISA. This error is amplified by the distance h, from the centroid of the set of markers to the ISA. In order to control it, it is not enough with increasing the accuracy of $\vec{\mathbf{w}}$, but it is necessary that the markers are arranged so that its centroid G is as close as possible to the ISA.

4. Application example

In order to show how the proposed method can be applied, we have developed an experiment to measure the kinematic screws of the trunk motions in seated posture. The main experiment is performed on a seated subject, which will describe the alternative motion of flexion and extension of the back. In order to obtain accurate measures of the ISA position, two devices for the external fixation of markers to the thorax and pelvis were designed (Fig. 4). The thoracic device consisted of a very light but rigid aluminium rod, bended forming a frame, on which the markers are located. This rod is placed in a semi-rigid plate with the form of the back. The plate is fixed on the back of the subject by means of elastic belts that are crossed on the chest. These belts are tightened so that there is no relative displacement between the system of markers and the thorax. A similar device has been designed for the pelvis movement analysis. This one is fixed to another plate placed below the iliac crests. The plate is fixed to the subject by means of a belt and a harness, to avoid displacements on the skin. In addition to the devices for the kinematic analysis other two markers of reference were placed on the subjects: one on the skin at L3 level and another one at T12 level.

Previous to this analysis a preliminary experiment was developed to analyze the accuracy of the measurement system. The upper back device was fixed on to a 50×50 cm board linked to a table by means of a hinge parallel to Y-axis. This device was adjusted on the board in such a way that the centroid of markers set was at approximately 1.5 cm from the hinge.

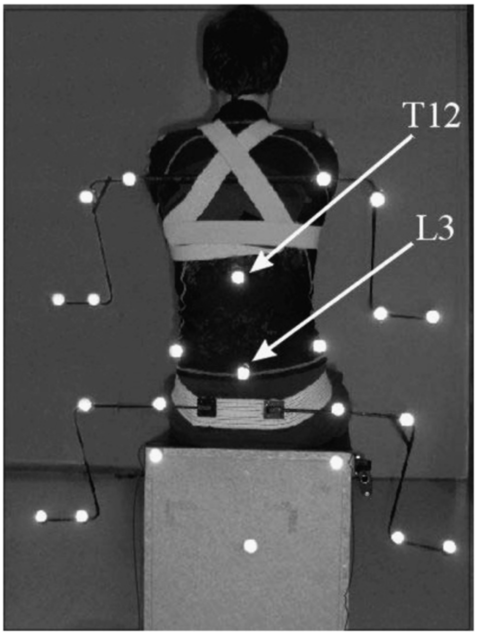

Fig. 4. Location of markers in thorax, pelvis and seat.

The board was moved in a rotation movement of approximately 90° from horizontal position to vertical position, in a forwards and backwards path. Co-ordinates of markers were registered with a passive marker stereophotogrammetric system (KINESCAN/IBV), with a sampling frequency of 25 frames per second. The registered co-ordinates were not smoothed. In order to minimize the error associated to low values of $|\vec{\mathbf{w}}|$, kinematic calculus were not developed from consecutive frames, but by spanning the time interval between frames and assigning the estimated value to the middle frame. A delay of 10 frames (0.36 s) was used. From these raw data, linear and angular velocities were calculated from finite differences. A threshold value of $\Omega > 6°$ between photograms was used in the ISA determination in order to avoid inaccuracies for small angular displacements at the beginning and at the end of motion. Experimental errors in linear and angular velocities were estimated as the residual between the measured values and the adjusted values by means of a local adjustment of cubical order, with a Gaussian weight function. The bandwidth of the Gaussian function was obtained so that the error autocorrelation was null. The same procedure was used to estimate experimental errors in markers coordinates.

Experimental error of ISA position was measured as shown in Fig. 3. The "true" ISA was estimated from the averaged value of the calculated $\vec{\mathbf{w}}(t)$ and $|\vec{\mathbf{r}}_{OH}(t)|$. As the movement was a pure rotation this averaging procedure ensures a good estimation of the ISA. Expected errors were calculated form expressions (26), (27) and (31)–(33).

Table 1 shows some relevant values of the expected and measured errors. As we can see, there is agreement between expected and measured errors. On the other hand, the accuracy of the device seems to be good in velocities and adequate in ISA position determination.

Although the analyzed motion in this experiment is a pure rotation, estimations of angular velocity of the body, velocity of the centroid $\vec{\mathbf{w}}'$ and location of the ISA are instantaneous values. So, the measured errors are a good estimation of the accuracy of measurement system in real cases. It could be possible to reduce these errors by means of a more effective smoothing data process, for example, by using spline functions or local regression.

For the main experiment, a similar procedure was followed. The coordinates of the markers were measured by using the same video–photogrammetry system. The raw measured values of the coordinates were smoothed by a local regression of cubical order, with a Gaussian weight function. The bandwidth of the Gaussian function was obtained separately, coordinate by coordinate, so that the error autocorrelation was null.

Table 1
Expected and measured errors

Variable	Measured error (standard deviation)	Expected error (standard deviation)
v_{G_X}	0.61 mm/s	0.62 mm/s
v_{G_Y}	0.26 mm/s	0.24 mm/s
v_{G_Z}	0.63 mm/s	0.62 mm/s
ω_X	0.0019 rad/s	0.0019 rad/s
ω_Y	0.0038 rad/s	0.0038 rad/s
ω_Z	0.0017 rad/s	0.0017 rad/s
OH_X	1.6 mm	2.1 mm
OH_Y	0.1 mm	0.0 mm
OH_Z	2.2 mm	2.1 mm

On the smoothed coordinates, the expressions for the kinematic analysis previously described are applied, calculating the components of the kinematic screws of the absolute motions of pelvis and thorax. From these two screws, the one corresponding to the thorax–pelvis relative movement was calculated, which is the relevant motion from the point of view of the raquis kinematics.

Two variables were calculated from the location of the ISA of the thorax–pelvis relative movement. The first one is the longitudinal displacement of the ISA along the raquis axis. The second one is the cross-sectional distance from the ISA to the back skin. These variables were measured from the projection of the intersection of ISA in the sagittal plane on the line defined by markers on L3 and T12 (Fig. 5).

Fig. 6 shows the evolution of the cross-sectional distance (see Fig. 5) of the ISA of thorax–pelvis relative motion during the cycles of flexion and extension. In the diagram, a scheme of lumbar vertebra in approximated scale has been superposed to illustrate the order of magnitude of the displacements. As can be seen, the cross-sectional position of the ISA is practically constant and remains in the top half of the vertebral body, as it has been described using X-rays in [9].

In Fig. 7 the longitudinal displacement (see Fig. 5) of the ISA throughout raquis lumbar based on the extension angle is shown. Also a scheme of lumbar raquis in approximated scale has been drawn, to illustrate the order of magnitude of the displacements. It can be seen that the longitudinal displacement takes place upwards in the motion of extension and downwards in the flexion one, with a range of about 8 cm.

This result demonstrates the sequential character of the motion of the different vertebral bodies, down upwards in the motion of extension and up downwards in the motion of flexion. In effect, the global movement of the thoracic box with respect to the pelvis is the sum of the screws of relative movement of each vertebra

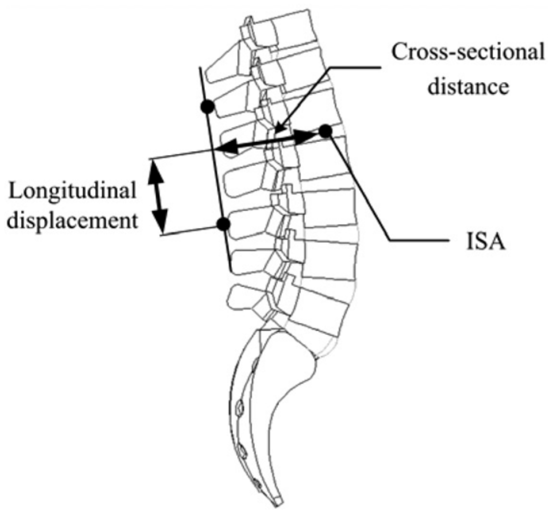

Fig. 5. Location of the ISA relative to local markers.

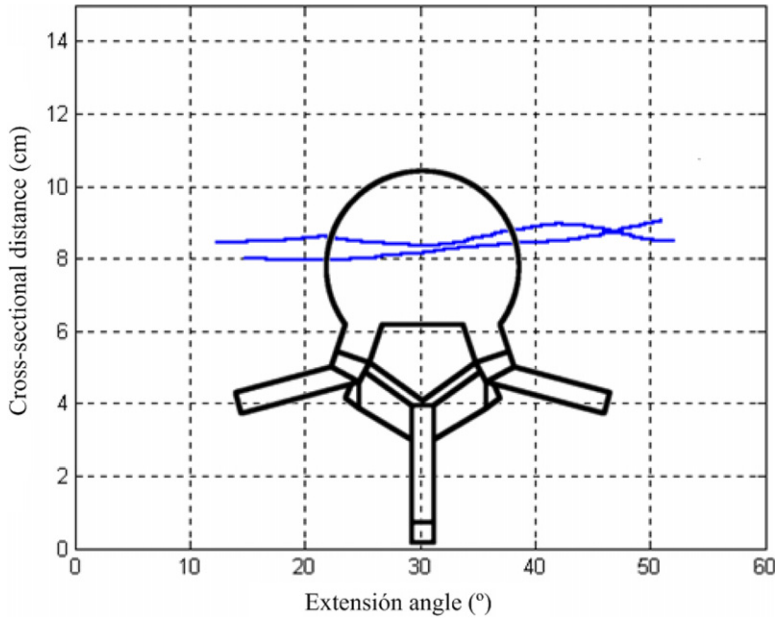

Fig. 6. Evolution of the cross-sectional distance of the ISA corresponding to the thorax–pelvis relative motion. A scheme of a lumbar vertebra in approximated scale is represented in order to show the order of magnitude of cross-sectional displacement.

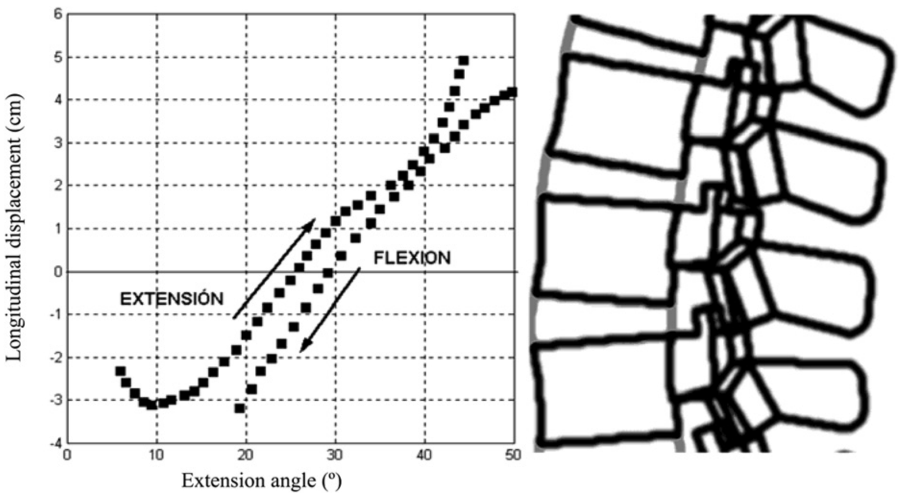

Fig. 7. Longitudinal displacement of ISA throughout lumbar raquis. A scheme of lumbar raquis in approximated scale is represented in order to show the order of magnitude of longitudinal displacement.

with respect to the lower vertebra. In the flexo-extension motion, these intervertebral motions can be represented by using a system of parallel screws with axes located on the half of intervertebral disc, approximately. The resultant of the system will be a parallel screw to the previous ones, whose position will fit with the centroid of the screws of intervertebral motion.

5. Conclusions

A new approach for kinematic analysis of corporal motions from kinetic and non-geometric considerations has been developed, which allows to obtain explicit expressions of the kinematic parameters and the experimental errors in its determination by using photogrammetry techniques.

A complete analysis of the random errors in the measurement of kinematic parameters has been developed, achieving explicit expressions of these based on the number of markers and their distribution, which allow to design systems of markers to keep the errors within an acceptable margin. This aspect is of great importance in the determination of the instantaneous screw axis, extraordinarily sensitive to the errors in the coordinates of the markers. The resulting expressions imply a substantial improvement compared with the present methods of estimation of errors, which are based on an isotropic distribution of markers, and which have been found to be unfeasible in realistic studies.

Acknowledgement

This research work has been partially funded by the Spanish Government Grant DPI2003-07883-C02-01.

References

[1] J. Angeles, E. Zakhariev, Computational Methods in Mechanical Systems: Mechanism Analysis, Synthesis, and Optimization, Springer, 1998, pp. 3–32.
[2] S. Ball, A Treatise on the Theory of Screw, Cambridge University Press, Cambridge, 1900, reprinted in 1998.
[3] O. Bottema, B. Roth, Theoretical Kinematics, Dover Publications Inc., New York, 1979.
[4] J.H. Challis, A procedure for determining rigid body transformation parameters, Journal of Biomechanics 28 (6) (1995) 733–737.
[5] P.P. Cheng, A.C. Nicol, J.P. Paul, Determination of axial rotation angles of limb segments, Journal of Biomechanics 33 (2000) 837–843.
[6] S.S.H.U. Gamage, J. Lasenby, New least squares solutions for estimating the average centre of rotation and the axis of rotation, Journal of Biomechanics 35 (2002) 87–93.
[7] S.-W. Lee, E. Draper, S. Hughes, Instantaneous center of rotation and instability of the cervical spine, Spine 22 (6) (1997) 641–648.
[8] C.G.M. Meskers et al., In vivo estimation of the glenohumeral joint rotation center from scapular bony landmarks by linear regression, Journal of Biomechanics 31 (1998) 93–96.
[9] A.A. White, M.M. Panjabi, Clinical Biomechanics of the Spine, Lippincott Williams & Wilkins, Philadelphia, 1990.
[10] H.J. Woltring, 3-D attitude representation of human joints: a standardization proposal, Journal of Biomechanics 27 (12) (1994) 1399–1414.
[11] H.J. Woltring, K. Long, P.J. Ostenbauer, A.W. Fuhr, Instantaneous helical axis estimation from 3-D video data in neck kinematics for whiplash diagnostics, Journal of Biomechanics 27 (12) (1994) 1415–1432.
[12] A. Cappozzo, U. Della Croce, A. Leardini, Lorenzo Chiari, Human movement analysis using stereophotogrammetry. Part 1. Theoretical background, Gait and Posture 21 (2005) 186–196.
[13] M.K. Keler, On the theory of screws and the dual method, in: Proceedings of a Symposium Commemorating the Legacy, Works and Life of Sir Robert Ball Upon the 100th Anniversaru of "A Treatise on the Theory of Screws", Cambridge, July 9–11, 2000.
[14] A.T. Yang, F. Freudenstein, Application of dual-number quaternion algebra to the analysis of spatial mechanism, Transactions of the ASME – Journal of Applied Mechanics, Series E 31 (1964) 300–308.
[15] G.R. Pennock, B.A. Oncu, Application of screw theory to rigid body dynamics, Transactions of the ASME – Journal of Dynamic Systems, Measurement and Control 114 (1992) 262–269.
[16] H. Stachel, Instantaneous spatial kinematics and the invariants of the axodes, in: Proceedings of a Symposium Commemorating the Legacy, Works and Life of Sir Robert Ball Upon the 100th Anniversaru of "A Treatise on the Theory of Screws", Cambridge, July 9–11, 2000.
[17] L. Chiari, U. Della Croce, A. Leardini, A. Cappozzo, Human Movement análisis using stereophotogrammetry. Part 2. Instrumental errors, Gait and Posture 21 (2005) 197–211.